



Refractory, Ceramic, and Composite Materials Тугоплавкие, керамические и композиционные материалы



UDC 666.9-129

https://doi.org/10.17073/1997-308X-2025-5-60-69

Research article Научная статья



Effect of spark plasma sintering temperature on the structure and properties of alumina ceramics containing barium hexaaluminate

K. A. Antropova, N. Yu. Cherkasova, N. S. Aleksandrova, R. R. Khabirov, A. A. Miller, M. Yu. Agafonov

Novosibirsk State Technical University 20 Karl Marks Prosp., Novosibirsk 630073, Russia

antropova.2017@stud.nstu.ru

Abstract. Alumina-based composite ceramics containing barium hexaaluminate are promising for various industrial applications, including the fabrication of replaceable cutting inserts. However, reports on such materials produced by spark plasma sintering (SPS) are scarce. This study aimed to evaluate the influence of sintering temperature on the structure and properties of alumina ceramics containing barium hexaaluminate. The materials were fabricated from highly dispersed Al₂O₃ and BaO powders by co-dispersion in an alcohol medium, followed by drying and spark plasma sintering at 1500, 1550, and 1600 °C. *X*-ray diffraction, scanning electron microscopy, and hydrostatic weighing were used to determine phase composition, microstructure, apparent density, and open porosity. Vickers hardness and fracture toughness were evaluated by indentation. The formation of α-Al₂O₃ and Ba_{0.83}Al₁₁O_{17.33} phases was confirmed. The relative density of alumina ceramics without additive reached 99.72 ± 0.3 %, while that of ceramics containing barium hexaaluminate was 92.45 ± 0.5 %. The average Al₂O₃ grain size decreased from 4.27 ± 1.80 μm (without additive) to 1.49 ± 0.80, 1.89 ± 0.85, and 1.60 ± 0.63 μm at sintering temperatures of 1500, 1550, and 1600 °C, respectively. The barium hexaaluminate plates grew with increasing temperature, from 2.45 ± 0.22 μm at 1500 °C to 5.23 ± 0.46 μm at 1600 °C. The maximum fracture toughness ($K_{\rm lc} = 5.00 \pm 0.10$ MPa·m^{1/2}) was obtained for the material containing barium hexaaluminate sintered at 1550 °C, which also exhibited a hardness of 2070 ± 43 HV₂.

Keywords: spark plasma sintering (SPS), alumina, barium hexaaluminate, phase formation, microstructure, fracture toughness

Acknowledgements: This research was funded by the Russian Science Foundation, grant No. 24-79-00256, https://rscf.ru/project/24-79-00256/. The experiments were carried out using the facilities of the Core Facilities Center "Structure, Mechanical and Physical Properties of Materials", Novosibirsk State Technical University (NSTU).

For citation: Antropova K.A., Cherkasova N.Yu., Aleksandrova N.S., Khabirov R.R., Miller A.A., Agafonov M.Yu. Effect of spark plasma sintering temperature on the structure and properties of alumina ceramics containing barium hexaaluminate. *Powder Metallurgy and Functional Coatings*. 2025;19(5):60–69. https://doi.org/10.17073/1997-308X-2025-5-60-69



Влияние температуры электроискрового спекания на структуру и свойства алюмооксидной керамики, содержащей гексаалюминат бария

К. А. Антропова , Н. Ю. Черкасова, Н. С. Александрова, Р. Р. Хабиров, А. А. Миллер, М. Ю. Агафонов

Новосибирский государственный технический университет

Россия, 630073, г. Новосибирск, пр-т Карла Маркса, 20

antropova.2017@stud.nstu.ru

Аннотация. Композиционная керамика на основе оксида алюминия, содержащая гексаалюминат бария, является перспективной для применения в различных областях промышленности, в том числе для изготовления сменных режущих пластин. Работ, в которых отмеченные материалы получены электроискровым спеканием, практически не наблюдается. Целью данного исследования являлась оценка влияния температуры электроискрового спекания на структуру и свойства керамики на основе оксида алюминия, содержащей гексаалюминат бария. Исследуемые материалы получены из высокодисперсных порошков оксида алюминия и оксида бария путем совместного диспергирования спиртовых суспензий, их сушки и последующего электроискрового спекания при температурах (t_c) 1500, 1550 и 1600 °C. Проводили рентгенофазовый анализ, исследования структуры методом растровой электронной микроскопии, оценку кажущейся плотности и открытой пористости методом гидростатического взвешивания. Оценивали твердость по Виккерсу и трещиностойкость методом индентирования. Зафиксировано формирование фаз α -Al $_2$ O $_3$ и Ba $_{0.83}$ Al $_{11}$ O $_{17.33}$. Относительная плотность от теоретической алюмооксидной керамики без добавок составляет 99.72 ± 0.3 %, при формировании гексаалюмината бария -92.45 ± 0.5 %. Средний размер зерен оксида алюминия в материале без добавки находится в диапазоне 4,27 ± 1,80 мкм, а при формировании 15 мас. % гексаалюмината бария -1.49 ± 0.80 , 1.89 ± 0.85 и 1.60 ± 0.63 мкм при $t_c = 1500$, 1550 и 1600 °C соответственно. Размеры пластин гексаалюмината бария с ростом температуры спекания увеличиваются. При $t_{\rm c}$ = 1500 °C их длина составляет $2,45\pm0,22$ мкм, а при $t_{c}=1600~{
m ^{\circ}C}-5,23\pm0,46$ мкм. Наиболее высокое значение критического коэффициента интенсивности напряжений $(5.00 \pm 0.10 \text{ M}\Pi a \cdot m^{1/2})$ зафиксировано для материала, содержащего гексаалюминат бария и спеченного при $t_c = 1550$ °C, твердость такого материала составляет $2070 \pm 43 \text{ HV}_2$.

Ключевые слова: электроискровое спекание, оксид алюминия, гексаалюминат бария, фазообразование, структура, трещиностойкость

Благодарности: Исследование выполнено за счет гранта Российского научного фонда No. 24-79-00256, https://rscf.ru/project/24-79-00256/. Исследования проведены на оборудовании ЦКП «Структура, механические и физические свойства материалов» НГТУ.

Для цитирования: Антропова К.А., Черкасова Н.Ю., Александрова Н.С., Хабиров Р.Р., Миллер А.А., Агафонов М.Ю. Влияние температуры электроискрового спекания на структуру и свойства алюмооксидной керамики, содержащей гексаалюминат бария. *Известия вузов. Порошковая металлургия и функциональные покрытия*. 2025;19(5):60–69. https://doi.org/10.17073/1997-308X-2025-5-60-69

Introduction

Research on alumina and alumina–zirconia ceramics continues to expand. Their combination of high mechanical performance and low weight, along with other advantageous properties, has driven adoption across medical [1], defence [2], and tooling [3] sectors. As performance requirements tighten, improving the service properties of oxide ceramics has become essential; in particular, boosting resistance to crack propagation remains a central challenge [4].

In modern materials science, an active approach is to reinforce alumina ceramics with alkali, alkaline-earth, and rare-earth metal hexaaluminates (MeAl $_{12}O_{19}$, magnetoplumbite; MeAl $_{11}O_{18}$, β -Al $_2O_3$)) [5]. In the struc-

ture of such materials, hexaaluminate grains are flattened hexagonal prisms that contribute to improved fracture toughness through various mechanisms [6–8]. The most frequently reported mechanisms include crack deflection, grain pull-out, crystal fracture in transverse – and less often longitudinal – directions, crack bridging, and crack branching. It has been noted that the overall material performance is significantly affected by the type of initial additive used for hexaaluminate formation [9] and on crystal size and volume fraction [6], which determine the strength of their bonding with the matrix grains and the mechanisms contributing to fracture toughness enhancement.

Numerous studies have reported that variations in hexaaluminate content lead to changes in key mate-



rial properties – such as density, porosity, hardness, strength, and fracture toughness. For instance, when up to 10 wt. % CaAl₁₂O₁₉ is formed in the structure of Al₂O₃–ZrO₂ ceramics, the fracture toughness increases from 5.8 to 6.3 MPa·m^{1/2}. Further increase in calcium hexaaluminate content results in a decrease in fracture toughness to 5.5 MPa·m^{1/2}, accompanied by reduced density and hardness [10]. A similar relationship was observed in [11], where the formation of 2.8 vol. % LaAl₁₁O₁₈ led to an increase in fracture toughness by approximately 1 MPa·m^{1/2}, whereas higher LaAl₁₁O₁₈ content reduced it to 2.7 MPa·m^{1/2}.

Notably, that hexaaluminates themselves exhibit a wide range of functional properties, including considerable catalytic activity and stability [12], luminescence [13], electrical conductivity [14], among others. Therefore, when selecting a hexaaluminate-forming additive for alumina ceramics, its choice should be guided by the intended application area. For example, calcium hexaaluminate is widely used in the production of medical ceramics [1]. The formation of barium hexaaluminate enhances thermal shock resistance, and compositions based on it remain among the least studied [8]. The relevance of researching the Al₂O₃-BaO system, along with its thermodynamic characteristics and the thermal stability of different phases, is discussed in the article [15]. It has also been reported that the barium hexaaluminate phase is the most thermally stable.

Barium hexaaluminate belongs to the β -Al $_2$ O $_3$ structural family and forms as nonstoichiometric phases such as Ba $_{0.75}$ Al $_{11}$ O $_{17.25}$, Ba $_{2.33}$ Al $_{21.33}$ O $_{34.33}$, and Ba $_{0.83}$ Al $_{11}$ O $_{17.33}$ [5; 16]. Due to its plate-like morphology, it also contributes to improving the fracture toughness of alumina ceramics. In [8] 20.89 vol. % Ba $_{0.75}$ Al $_{11}$ O $_{17.25}$ in an Al $_2$ O $_3$ -ZrO $_2$ matrix increased fracture toughness by approximately 25 % relative to the additive-free material. Further increase in content to 41.38 vol. % yielded a smaller additional gain in toughness but markedly reduced hardness, strength, and density. Similar plate-mediated toughening has been reported for Al $_2$ O $_3$ with up to 10 vol. % ZrO $_2$ [17], with effectiveness of toughness enhancement tied to the degree of material densification.

This study examines the effect of spark plasma sintering (SPS) parameters on the structure and properties of alumina ceramics with barium oxide additive. As noted in [3], spark plasma sintering enables the fabrication of ceramic workpieces for cutting-tool production. Therefore, the present work not only contributes to the body of knowledge on the Al_2O_3 –BaO system but may also hold practical significance for developments in the tooling industry.

Materials and methods

High-purity alumina powder (99 %, average particle size 140 ± 50 nm, China) and barium oxide powder (99 %, average particle size 2.7 ± 0.6 µm, Russia; prepared in accordance with TU 6-09-5397-88) were used as starting materials. Alcohol suspensions were prepared using isopropyl alcohol (50 vol. %) as a dispersion medium for mixing the initial powders. The BaO content was set to 3 wt. % to form approximately 15 wt. % barium hexaaluminate. A relatively high barium hexaaluminate fraction was chosen to clearly evaluate its effect on the properties of the studied materials.

Dispersion was carried out in a ball mill for 10 h with periodic stops to cool the suspension. The rotation speed was 90 rpm. The drum of the mill was lined with polypropylene, and alumina grinding bodies 3 mm in diameter were used.

After dispersion, the powders were dried and consolidated by spark plasma sintering on an MS-1 unit at sintering temperatures (t_s) of 1500–1600 °C, under a pressure of 17 MPa, with a 5-minute holding time at maximum temperature. To prevent direct interaction between the powder and the tooling surfaces, graphite paper was placed between the powder and the die walls, as well as between the powder and the punch faces. Heating was provided by pulsed direct current passing through the graphite tooling. The temperature was measured using a pyrometer positioned in a side hole of the die assembly.

The apparent density and open porosity of the sintered materials were determined by the hydrostatic weighing method.

The apparent density was calculated as the ratio of the dry sample mass to the difference between the saturated and immersed masses:

$$\rho_{\rm app} = \frac{M_{\rm dry}}{M_{\rm sat} - M_{\rm lig}} \ [\rm g/cm^3],$$

where $M_{\rm dry}$ is the mass of the dry sample, g; $M_{\rm sat}$ is the mass of the sample saturated with liquid, g; $M_{\rm liq}$ is the mass of the sample immersed in liquid, g.

The relative density was calculated as

$$\rho_{rel} = \frac{\rho_{app}}{\rho_{theor}} \cdot 100 \%.$$

The theoretical density was determined using the literature values of the *X*-ray densities of the sintered components according to the formula:

$$\rho_{\text{theor}} = \left(\frac{m_i}{\rho_i} + \frac{m_n}{\rho_n}\right)^{-1} \cdot 100 \% [g/\text{cm}^3],$$



where ρ_i and ρ_n are the theoretical densities of the individual components, g/cm³; m_i and m_n are their mass fractions in the composite, %.

The open porosity (P_0) was calculated as

$$P_{\rm o} = \frac{M_{\rm sat} - M_{\rm dry}}{M_{\rm sat} - M_{\rm lio}} \cdot 100 \%.$$

X-ray diffraction (XRD) analysis was performed using a PowDix600 diffractometer (ADWIN Smart Factory, Republic of Belarus) with $CuK_{\alpha_{1,2}}$ radiation. The phases were identified using the ICDD PDF-4+ database. Polished sections for microstructural analysis were prepared using standard procedures, including grinding and polishing with diamond wheels and suspensions of various fineness. To reveal the grain structure, thermal etching was performed at a temperature 200 °C below the sintering temperature. Microstructural analysis was carried out using an EVO 50 scanning electron microscope (Carl Zeiss, Germany) equipped with an X-ray microanalysis attachment. Prior to examination, the polished sections were coated with a 40-nm copper layer to improve conductivity. Secondary electron detection was used for imaging. Grain sizes were measured using the JMicroVision 1.3.4 software. The alumina grain size was determined as the equivalent-circle diameter corresponding to the grain projection area in the microstructure image. For barium hexaaluminate grains, their length and width were measured, and the aspect ratio was calculated. At least 300 alumina grains and 100 barium hexaaluminate grains were analyzed for each composition.

The Vickers hardness and fracture toughness were evaluated by the indentation method under a 2-kg load using an SV-50A Vickers hardness tester (China). The fracture toughness, $K_{\rm Ic}$ (critical stress intensity factor), was calculated using the following equation [18]:

$$K_{\rm Ic} = 0.048 \left(\frac{c}{a}\right)^{-0.5} \left(\frac{HV}{E\Phi}\right)^{-0.4} \frac{HVa^{0.5}}{\Phi} [{\rm MPa \cdot m^{1/2}}],$$

where HV is the hardness, GPa; a is the half-diagonal of the indentation, μ m; c is the length of the radial crack measured from the indentation center, μ m; $\Phi = 3$ is the constant.

The Young's modulus (*E*) of the composite materials was estimated by the rule of mixtures:

$$E = \left(\frac{m_i}{E_i} + \frac{m_j}{E_j}\right)^{-1} \cdot 100 \% \text{ [GPa]},$$

where E_i and E_j are the Young's moduli of Al_2O_3 (397 GPa) and $Ba_{0.83}Al_{11}O_{17.33}$ (226 GPa), respectively;

 m_i and m_j are their mass fractions (%). The modulus values were taken from the literature [19].

Results and discussion

Experimental materials were sintered from starting mixtures of alumina and barium oxide. The sintering temperature (t_s) was 1500, 1550, and 1600 °C. As a reference, an additive-free alumina ceramics was prepared.

X-ray diffraction patterns of the sintered materials are shown in Fig. 1. Regardless of the sintering temperature, the materials with BaO in the starting mixture display, in addition to α -Al₂O₃, diffraction peaks of Ba_{0.83}Al₁₁O_{17.33}. No other barium-containing phases were detected.

The apparent density and open porosity of the sintered materials were evaluated; the results are summarized in Table 1. The highest relative density (with respect to the theoretical density) was obtained for the additive-free alumina ceramics. Formation of barium hexaaluminate in the composite led to a decrease in relative density and an increase in open porosity, which is consistent with prior reports on hexaaluminate formation in alumina matrix [5; 11]. With increasing sintering temperature, density and porosity changed nonlinearly.

Microstructural studies were performed by scanning electron microscopy (SEM). In the SEM micro-

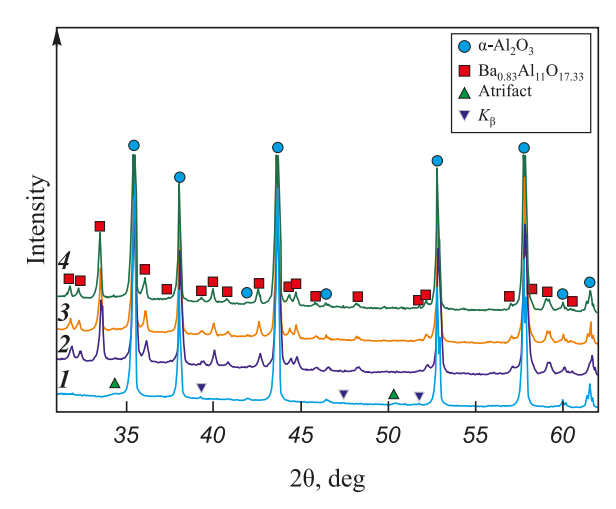


Fig. 1. X-ray patterns of the sintered materials 1 – alumina ceramics without additives, sintered at $t_s = 1500$ °C; 2–4 – ceramics of the composition Al₂O₃ + Ba_{0.83}Al₁₁O_{17.33} ceramics, sintered at $t_s = 1500$ (2), 1550 (3), and 1600 (4) °C

Рис. 1. Рентгеновские дифрактограммы спеченных исследуемых материалов *1* – алюмооксидная керамика без добавок,

спеченная при $t_{\rm c}=1500~{\rm ^{\circ}C}$; 2—4 — керамика состава ${\rm Al_2O_3+Ba_{0.83}Al_{11}O_{17.33}}$, спеченная при $t_{\rm c}=1500~(2),1550~(3)$ и $1600~(4)~{\rm ^{\circ}C}$



Table 1. Apparent density and open porosity of the sintered materials	
Таблица 1. Кажущаяся плотность и открытая пористость спеченных материалов	

Material	Sintering temperature, °C	Apparent density, g/cm ³	Relative density, % of theoretical	Open porosity, %
Al_2O_3	1500	3.98 ± 0.02	99.72 ± 0.3	0.26 ± 0.07
	1500	3.70 ± 0.04	92.45 ± 0.5	4.75 ± 0.09
$Al_2O_3 + Ba_{0.83}Al_{11}O_{17.33}$	1550	3.86 ± 0.03	96.41 ± 0.4	1.76 ± 0.08
	1600	3.86 ± 0.03	96.35 ± 0.4	2.08 ± 0.08

graphs (Fig. 2), the darker equiaxed grains correspond to the low-Z alumina phase, whereas the brighter elongated grains belong to the Ba-rich phase. SEM-EDS spot analyses conducted on the elongated grains confirmed the presence of Ba, Al, and O, identifying them as barium hexaaluminate (Fig. 2, e). Grains of both

phases are distributed fairly uniformly, though local clusters of bright elongated grains are occasionally observed.

A detailed quantitative analysis of the structural constituents was performed, and the results are presented in Fig. 3 and Table 2. The average grain size of alu-

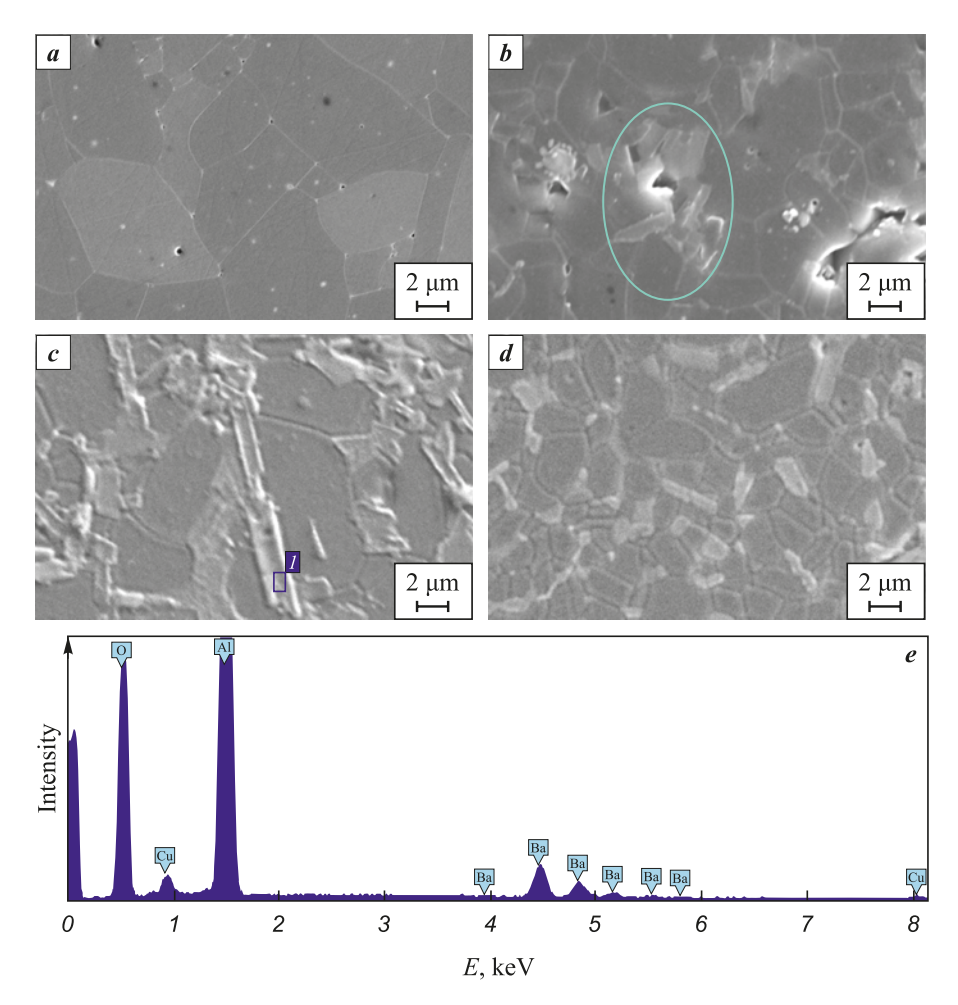


Fig. 2. Microstructure of the sintered materials

a – alumina ceramics without additives; b–d – ceramics containing barium hexaaluminate sintered at t_s , °C – 1500 (b), 1550 (c), 1600 (d); e – results of micro-X-ray spectral analysis obtained from region I marked in Fig. 2, c

Рис. 2. Структура спеченных материалов

 \pmb{a} – алюмооксидная керамика без добавок; \pmb{b} – \pmb{d} – содержащая гексаалюминат бария; $t_{\rm c}$, °С – 1500 (\pmb{b}), 1550 (\pmb{c}), 1600 (\pmb{d}); \pmb{e} – результаты микрорентгеноспектрального анализа, полученные с области \pmb{I} , выделенной на рис. 2, \pmb{c}

Antropova K.A., Cherkasova N.Yu., and etc. Effect of spark plasma sintering temperature ...

mina in the additive-free material was 4.27 ± 1.80 µm. The alumina powder used in this study was highly dispersed, which provided high sinterability. In addition, the SPS technique and the presence of barium oxide contributed to the intensification of the sintering process. In materials containing BaO, the alumina grains were significantly smaller. For instance, under identical sintering conditions at $t_s = 1500$ °C, the alumina grain size decreased by about 65 % in the material containing barium hexaaluminate. This effect can be attributed to Ba segregation along alumina grain boundaries, which inhibits their migration and growth [20]. Furthermore, the growth of hexaaluminate grains of any chemical composition is usually accompanied by the consumption of alumina grains, which also leads

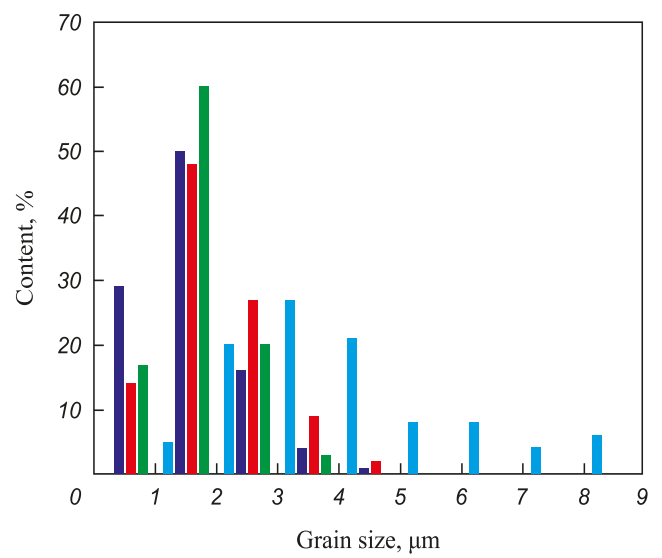
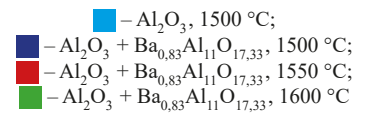


Fig. 3. Grain size distribution of alumina in the sintered materials

 $\begin{array}{c} -\operatorname{Al}_2\operatorname{O}_3,\ 1500\ ^\circ\mathrm{C};\\ -\operatorname{Al}_2\operatorname{O}_3 + \operatorname{Ba}_{0.83}\operatorname{Al}_{11}\operatorname{O}_{17.33},\ 1500\ ^\circ\mathrm{C};\\ -\operatorname{Al}_2\operatorname{O}_3 + \operatorname{Ba}_{0.83}\operatorname{Al}_{11}\operatorname{O}_{17.33},\ 1550\ ^\circ\mathrm{C};\\ -\operatorname{Al}_2\operatorname{O}_3 + \operatorname{Ba}_{0.83}\operatorname{Al}_{11}\operatorname{O}_{17.33},\ 1600\ ^\circ\mathrm{C} \end{array}$

Рис. 3. Распределение размеров зерен оксида алюминия в спеченных материалах



to their size reduction – a behavior consistent with previously reported findings [21; 22].

The alumina ceramics exhibited the widest grain size distribution, whereas in the material containing barium hexaaluminate and sintered at $t_s = 1600 \,^{\circ}\text{C}$, the distribution of Al₂O₃ grains was the narrowest, with a maximum grain size not exceeding 4 μm. It was also observed that the barium hexaaluminate plates increased in size with rising sintering temperature. At $t_s = 1600$ °C, both the length and width of the hexaaluminate plates increased. The aspect ratio of the barium hexaaluminate grains changed nonlinearly, reaching its minimum value at $t_s = 1550$ °C. This indicates that at the maximum sintering temperature, the most intensive growth of barium hexaaluminate plates occurs, accompanied by alumina grain consumption, which ultimately results in smaller alumina grains. Therefore, at $t_s = 1600$ °C, the decrease in alumina grain size is mainly associated with their participation in barium hexaaluminate formation rather than Ba segregation along grain boundaries.

The observed grain-structure features correlate with the changes in density and porosity of the studied materials. It was established that pores in the composite ceramics are predominantly concentrated in regions where barium hexaaluminate grains accumulate (highlighted by an oval in Fig. 2, b). Hence, the presence of pores is associated with the loose packing of platelike grains, which explains the pronounced decrease in density and increase in porosity upon BaO addition in the materials sintered at $t_s = 1500$ °C. Further temperature increase promoted alumina grain growth. At $t_s = 1550$ °C, the average Al₂O₃ grain size reached approximately $1.89 \pm 0.85 \mu m$. The coarsening of alumina grains led to a reduction in open porosity and an increase in relative density. At this temperature, alumina grain growth likely inhibited the elongation of barium hexaaluminate plates. However, at $t_s = 1600$ °C, the growth of barium hexaaluminate plates dominated, resulting in longer plates, smaller alumina grains, and increased porosity.

Table 2. Grain sizes of the sintered materials
Таблица 2. Размеры зерен спеченных материалов

	Sintering	Average Al ₂ O ₃ grain size, μm	Ba _{0.83} Al ₁₁ O _{17.33} grains		
Material	temperature, °C		Length, µm	Width, μm	Aspect ratio
Al_2O_3	1500	4.27 ± 1.80	_	_	_
	1500	1.49 ± 0.80	2.45 ± 0.22	0.57 ± 0.05	1.0:4.3
$Al_2O_3 + Ba_{0.83}Al_{11}O_{17.33}$	1550	1.89 ± 0.85	3.38 ± 0.21	0.93 ± 0.04	1.0:3.6
	1600	1.60 ± 0.63	5.23 ± 0.46	1.20 ± 0.06	1.0:4.4



Plate-like grains in the microstructure can significantly influence the mechanical properties of the material [19]. The results of Vickers hardness and fracture toughness measurements are summarized in Table 3. The materials containing barium hexaaluminate exhibited higher hardness compared with the additive-free alumina ceramics. For oxide ceramics, the incorporation of hexaaluminates more commonly results in hardness degradation [9–11]; in this case, however, the hardness increase is attributed to the substantial refinement of alumina grains. An improvement in fracture toughness was also observed in alumina ceramics containing barium hexaaluminate. The highest $K_{\rm LC}$ value was recorded for the material sintered at $t_s = 1550$ °C. It is likely that this composition provides the most favorable combination of porosity and grain sizes of both alumina and barium hexaaluminate.

Fig. 4 shows a typical Vickers indentation with radial cracks emerging from the indentation diagonals

and a magnified view of a crack propagating through the Al_2O_3 –Ba $Al_{12}O_{19}$ composite. The measured crack lengths, taken from the indentation center to the crack tip, correlate with the calculated K_{1c} value. In the additive-free alumina, the average crack length reaches ~80 μ m, whereas in the composite ceramics it ranges from 50 to 55 μ m, with the maximum length not exceeding 65 μ m.

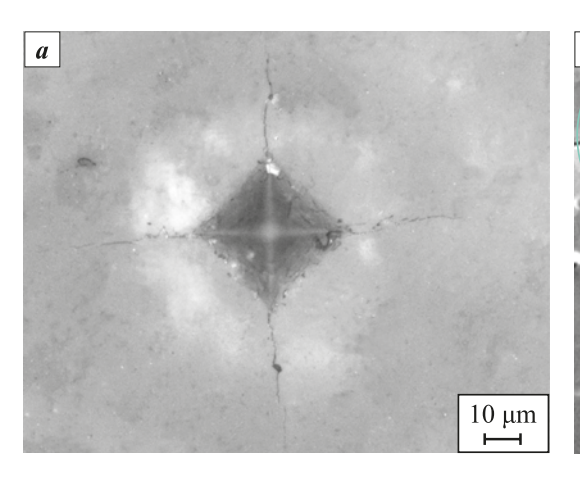
Detailed examination of the crack path (Fig. 4, b) revealed intergranular fracture along alumina grain boundaries and transgranular fracture of barium hexaaluminate plates in both transverse (I) and longitudinal (2) sections. Crack propagation was further accompanied by deflection at plate interfaces and the formation of crack bridging (3).

Conclusions

1. Regardless of the sintering temperature, XRD analysis of materials containing barium oxide in

Table 3. Hardness and fracture toughness of the investigated materials Таблица 3. Твердость и трещиностойкость исследуемых материалов

Material			Fracture toughness, MPa·m ^{1/2}	
Al_2O_3	1500	1990 ± 71	4.65 ± 0.14	
${\bf Al_2O_3 + Ba_{0.83}Al_{11}O_{17.33}}$	1500	2085 ± 33	4.85 ± 0.08	
	1550	2070 ± 43	5.00 ± 0.10	
	1600	2120 ± 67	4.50 ± 0.18	



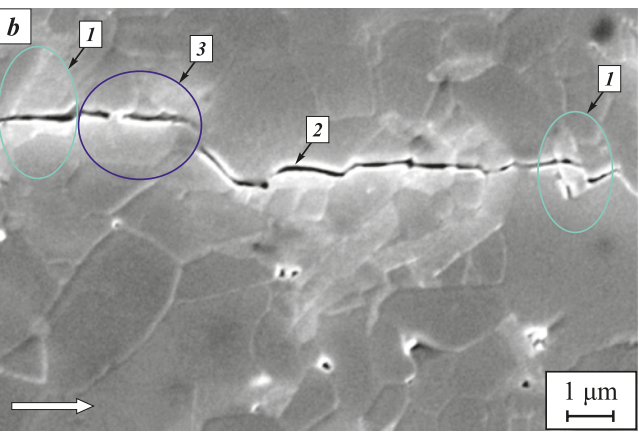


Fig. 4. Typical indentation (a) and propagating crack (b) in the investigated materials containing barium hexaaluminate

Numbers indicate the toughening mechanisms: I – plate fracture in the transverse direction;

2 – in the longitudinal direction with subsequent crack path deflection; 3 – crack bridging

The white arrow indicates the direction of crack propagation

Рис. 4. Типичный снимок отпечатка (a) и распространяющейся трещины (b) в исследуемых материалах, содержащих гексаалюминат бария

Цифрами обозначены механизмы повышения трещиностойкости: I – перерезание пластины в поперечном направлении; 2 – в продольном направлении с последующим отклонением траектории распространения; 3 – формирование мостиков



the starting mixture revealed, in addition to α -Al₂O₃, the presence of Ba_{0.83}Al₁₁O_{17.33} reflections.

- 2. The formation of barium hexaaluminate leads to a decrease in relative density and an increase in open porosity. With rising sintering temperature, density and porosity change non-uniformly due to the simultaneous growth and loose packing of plate-like bariumhexaaluminate grains and variation in alumina grain size.
- 3. The size of barium-hexaaluminate plates increases with sintering temperature: their average length rises from 2.45 \pm 0.22 μm at 1500 °C to 5.23 \pm 0.46 μm at 1600 °C.
- 4. The formation of barium hexaaluminate in the ceramic microstructure causes a reduction of alumina grain size by approximately 65 % under identical sintering conditions at $t_s = 1500$ °C.
- **5.** The highest fracture toughness $(K_{\rm Ic} = 5.00 \pm$ $\pm 0.10 \text{ MPa} \cdot \text{m}^{1/2}$) was obtained for the material containing barium hexaaluminate and sintered at $t_s = 1550$ °C. The corresponding Vickers hardness was $2070 \pm 43 \text{ HV}_{2}$.

References / Список литературы

- Podzorova L.I., Volchenkova V.A., Il'icheva A.A., Andreeva N.A., Konovalov A.A., Penkina T.N., Pen'kova O.I. Chemical composition stability of corundum/zirconium dioxide composites in a biological media. Inorganic Materials: Applied Research. 2024;15(4):983-987. https://doi.org/10.1134/S2075113324700497
- Garshin A.P., Kulik V.I., Nilov A.S. Shock-resistant materials based on commercial grade ceramic: achievements and prospects for improving their ballistic efficiency. Refractories and Industrial Ceramics. 2016;57(2):207-219. https://doi.org/10.1007/s11148-016-9955-0
- Kuzin V.V., Grigor'ev N., Fedorov S.Y., Volosova M.A., Pinargote N.V.S. Spark plasma sintering of Al₂O₃-ceramic workpieces for small end milling cutters. Refractories and Industrial Ceramics. 2019;59(6):623-627. https://doi.org/10.1007/s11148-019-00285-2
- Abyzov A.M. Aluminum oxide and alumina ceramics (review). Part 1. Properties of Al₂O₃ and commercial production of dispersed Al₂O₃. Refractories and Industrial Ceramics. 2019;60(1):24-32. https://doi.org/10.1007/s11148-019-00304-2
- Tian M., Wang X.D., Zhang T. Hexaaluminates: a review of the structure, synthesis and catalytic performance. *Catalysis Science & Technology*. 2016;6(7):1984–2004. https://doi.org/10.1039/C5CY02077H
- Kern F. A comparison of microstructure and mechanical properties of 12Ce-TZP reinforced with alumina and in situ formed strontium- or lanthanum hexaaluminate precipitates. Journal of the European Ceramic Society. 2014;34(2):413-423. https://doi.org/10.1016/j.jeurceramsoc.2013.08.03 7

- Shi S., Cho S., Goto T., Sekino T. Role of CeAl, O, in reinforcing Al₂O₂/Ti composites by adding CeO₂. International Journal of Applied Ceramic Technology. 2021;18(1):170–181. https://doi.org/10.1111/ijac.13629
- Liu L., Takasu Y., Onda T., Chen Z.-C. Influence of in-situ formed Ba-β-Al₂O₃ on mechanical properties and thermal shock resistance of ZTA/Ba-β-Al₂O₃ composites. Ceramics International. 2020;46(3):3738-3743. https://doi.org/10.1016/j.ceramint.2019.10.095
- Rivero-Antúnez P., Morales-Flórez V., Cumbrera F.L., Esquivias L. Rietveld analysis and mechanical properties of in situ formed La-β-Al₂O₂/Al₂O₂ composites prepared by sol-gel method. Ceramics International. 2022; 48(17):24462-24470. https://doi.org/10.1016/j.ceramint.2022.05.058
- 10. Sktani Z.D.I., Azhar A.Z.A., Ratnam M.M., Ahmad Z.A. The influence of in-situ formation of hibonite on the properties of zirconia toughened alumina (ZTA) composites. Ceramics International. 2014;40(4):6211–6217. https://doi.org/10.1016/j.ceramint.2013.11.076
- 11. Negahdari Z., Willert-Porada M., Pfeiffer C. Mechanical properties of dense to porous alumina/lanthanum hexaaluminate composite ceramics. Materials Science and Engineering: A. 2010;527(12):3005-3009. https://doi.org/10.1016/j.msea.2010.01.050
- 12. Kerzhentsev M.A., Podyacheva O.Yu., Shikina N.V., Mishanin S.V., Ismagilov Z.R., Deutschmann O., Russo G. Application of catalytic technologies for power plants based on high-temperature fuel cells. Chemistry for Sustainable Development. 2021;29(3):317-324. https://doi.org/10.15372/CSD2021309
 - Керженцев М.А., Подъячева О.Ю., Шикина Н.В., Мишанин С.В., Исмагилов З.Р., Deutschmann O., Russo G. Применение каталитических технологий для энергоустановок на высокотемпературных топливных элементах. Химия в интересах устойчивого развития. 2021;29(3):326-333. https://doi.org/10.15372/KhUR2021309
- 13. Selyunina L.A., Mishenina L.N., Slizhov Y.G., Kozik V.V. Effect of citric acid and ethylene glycol on the formation of calcium aluminate via the sol-gel method. Russian Journal of Inorganic Chemistry. 2013;58(4):450–455. https://doi.org/10.1134/S0036023613040165
 - Селюнина Л.А., Мишенина Л.Н., Слижов Ю.Г., Козик В.В. Влияние лимонной ксилоты и этиленгликоля на формирование алюмината кальция золь-гель методом. Журнал неорганической химии. 2013;58(4): 517-522. https://doi.org/10.7868/S0044457X1304017X
- 14. Zhdanok A.A., Berdnikova L.K., Korotaeva Z.A., Tolochko B.P., Bulgakov V.V., Mikhaylenko M.A. Specifics of obtaining a vacuum-tight weakly conductive ceramics based on barium aluminate. Refractories and Industrial Ceramics. 2023;64(4):407-412.

https://doi.org/10.1007/s11148-024-00861-1

Жданок А.А., Бердникова Л.К., Коротаева З.А., Толочко Б.П., Булгаков В.В., Михайленко М.А. Особенности получения вакуум-плотной слабопроводящей кера-



мики на основе алюмината бария. *Новые огнеупоры*. 2023;(8):14–20.

https://doi.org/10.17073/1683-4518-2023-8-14-20

- Tyurnina N.G., Lopatin S.I., Balabanova E.A., Shugurov S.M., Tyurnina Z.G., Polyakova I.G. Thermodynamic properties of the BaO–Al₂O₃ system. *Journal of Alloys and Compounds*. 2023;969:172266. https://doi.org/10.1016/j.jallcom.2023.172266
- 16. Nugroho S., Chen Z.-C., Kawasaki A., Jarligo M.O.D. Solid-state synthesis and formation mechanism of barium hexaaluminate from mechanically activated Al₂O₃–BaCO₃ powder mixtures. *Journal of Alloys and Compounds*. 2010;502(2):466–471. https://doi.org/10.1016/j.jallcom.2010.04.198
- 17. Liu L., Maeda K., Onda T., Chen Z.-C. Effect of YSZ with different Y₂O₃ contents on toughening behavior of Al₂O₃/Ba-β-Al₂O₃/ZrO₂ composites. *Ceramics International*. 2019;45(14):18037–18043. https://doi.org/10.1016/j.ceramint.2019.06.023
- **18.** Niihara K., Morena R., Hasselman D.P.H. Evaluation of K_{Ic} of brittle solids by the indentation method with low crack-to-indent ratios. *Journal of Materials Science Let*-

- *ters*. 1982;1(1):13–16. https://doi.org/10.1007/BF00724706
- **19.** Chen Z., Chawla K., Koopman M. Microstructure and mechanical properties of in situ synthesized alumina/Ba–β-alumina/zirconia composites. *Materials Science and Engineering: A.* 2004;367(1–2):24–32. https://doi.org/10.1016/j.msea.2003.09.070
- Altay A., Gülgün M.A. Microstructural evolution of calcium-doped α-alumina. *Journal of the American Ceramic Society*. 2003;86(4):623–629. https://doi.org/10.1111/j.1151-2916.2003.tb03349.x
- 21. Rani D.A., Yoshizawa Y., Hirao K., Yamauchi Y. Effect of rare-earth dopants on mechanical properties of alumina. *Journal of the American Ceramic Society*. 2004;87(2):289–292. https://doi.org/10.1111/j.1551-2916.2004.00289.x
- 22. Sktani Z.D.I., Rejab N.A, Rosli A.F.Z, Arab A., Ahmad Z.A. Effects of La₂O₃ addition on microstructure development and physical properties of harder ZTA–CeO₂ composites with sustainable high fracture toughness. *Journal of Rare Earths*. 2021;39(7):844-849. https://doi.org/10.1016/j.jre.2020.06.005

Information about the Authors



Сведения об авторах

Kristina A. Antropova – Junior Researcher, Research Laboratory of Physical and Chemical Technologies and Functional Materials, Novosibirsk State Technical University (NSTU)

(D) ORCID: 0000-0001-5482-3537

E-mail: antropova.2017@stud.nstu.ru

Nina Yu. Cherkasova – Cand. Sci. (Eng.), Senior Researcher, Research Laboratory of Physical and Chemical Technologies and Functional Materials, NSTU

(D) ORCID: 0000-0002-5603-7852

E-mail: cherkasova.2013@corp.nstu.ru

Natalya S. Aleksandrova – Junior Researcher, Research Laboratory of Physical and Chemical Technologies and Functional Materials, NSTU

(D) ORCID: 0000-0002-7619-525X

E-mail: aleksandrova.2017@corp.nstu.ru

Roman R. Khabirov – Junior Researcher, Center for Technological Excellence, NSTU

(D) ORCID: 0000-0003-4720-2876

🚾 E-mail: xabirov.2016@stud.nstu.ru

Aleksandr A. Miller – Master's Student, Department of Materials Science in Mechanical Engineering, NSTU

(D) ORCID: 0009-0008-0534-0879

E-mail: miller.2020@stud.nstu.ru

Mikhail Yu. Agafonov – Master's Student, Department of Materials Science in Mechanical Engineering, NSTU

(D) ORCID: 0009-0008-8153-9118

E-mail: agafonov.2020@stud.nstu.ru

Кристина Александровна Антропова – мл. науч. сотрудник научно-исследовательской лаборатории физико-химических технологий и функциональных материалов Новосибирского государственного технического университета (НГТУ)

(D) ORCID: 0000-0001-5482-3537

E-mail: antropova.2017@stud.nstu.ru

Нина Юрьевна Черкасова – к.т.н., ст. науч. сотрудник научноисследовательской лаборатории физико-химических технологий и функциональных материалов НГТУ

D ORCID: 0000-0002-5603-7852

E-mail: cherkasova.2013@corp.nstu.ru

Наталья Сергеевна Александрова – мл. науч. сотрудник научно-исследовательской лаборатории физико-химических технологий и функциональных материалов НГТУ

(D) ORCID: 0000-0002-7619-525X

E-mail: aleksandrova.2017@corp.nstu.ru

Роман Рафаэлович Хабиров – мл. науч. сотрудник Центра технологического превосходства НГТУ

(D) ORCID: 0000-0003-4720-2876

E-mail: xabirov.2016@stud.nstu.ru

Александр Андреевич Миллер – магистрант кафедры материаловедения в машиностроении НГТУ

(D) ORCID: 0009-0008-0534-0879

🗷 **E-mail:** miller.2020@stud.nstu.ru

Михаил Юрьевич Агафонов – магистрант кафедры материаловедения в машиностроении НГТУ

(D) ORCID: 0009-0008-8153-9118

E-mail: agafonov.2020@stud.nstu.ru

Antropova K.A., Cherkasova N.Yu., and etc. Effect of spark plasma sintering temperature ...

Contribution of the Authors



Вклад авторов

- *K. A. Antropova* defined the research objectives, conducted the experiments, and wrote the manuscript.
- *N. Yu. Cherkasova* developed the concept and defined the objectives of the study, and contributed to writing the manuscript.
- *N. S. Aleksandrova* performed *X*-ray phase analysis, and participated in the discussion of the results.
- *R. R. Khabirov* carried out structural studies and participated in the discussion of the results.
- **A. A. Miller** prepared the mixtures and experimental samples, and participated in discussions of the results.
- *M. Yu. Agafonov* conducted the investigations and participated in the discussion of the results.

- *К. А. Антропова* определение цели работы, проведение экспериментов, написание статьи.
- **Н. Ю. Черкасова** определение концепции и цели работы, написание статьи.
- **Н. С. Александрова** проведение рентгенофазового анализа, участие в обсуждении результатов.
- *Р. Р. Хабиров* проведение структурных исследований, участие в обсуждении результатов.
- **А. А. Миллер** приготовление смесей и экспериментальных образцов, участвие в обсуждении результатов.
- **М. Ю. Агафонов** проведение исследований, участие в обсуждении результатов.

Received 14.03.2025 Revised 25.04.2025 Accepted 28.04.2025 Статья поступила 14.03.2025 г. Доработана 25.04.2025 г. Принята к публикации 28.04.2025 г.